Published in final edited form as:
Bioconjug Chem. 2009 February ; 20(2): 213–221. doi:10.1021/bc800237t.

HPMA Polymer-based Site-specific Delivery of Oligonucleotides to Hepatic Stellate Cells

Ningning Yang, **Zhaoyang Ye**, **Feng Li**, and **Ram I. Mahato***
Department of Pharmaceutical Sciences, University of Tennessee, Health Science Center, Memphis, TN 38103

Abstract

The objective was to determine whether bioconjugation of type I collagen specific triplex forming oligonucleotide (TFO) to N-(2-hydroxypropyl) methacrylamide (HPMA) containing tetrapeptide Gly-Phe-Leu-Gly (GFLG) and mannose 6-phosphate (M6P) can provide their targeted delivery to hepatic stellate cells (HSCs). Following bioconjugation, M6P-GFLG-HPMA-GFLG-^{32}P-TFO was characterized by PAGE, HPLC and GPC, and then its biodistribution was determined. TFO was dissociated from the conjugate when incubated with papain and formed triplex with the target DNA duplex. Type 1 collagen gene expression was significantly inhibited when HSC-T6 cells were transfected with this conjugate. Following tail vein injection into rats, M6P-GFLG-HPMA-GFLG-^{32}P-TFO was rapidly cleared from the circulation and accumulated mainly in the liver. The plasma concentration versus time profile was biphasic, with 12.37 min as $t_{1/2}$ of distribution and 2886.48 min as $t_{1/2}$ of elimination. A large proportion of the injected M6P-GFLG-HPMA-GFLG-^{32}P-TFO was taken up by the HSCs of both normal and fibrotic rats, which were isolated by liver perfusion at 30 min post injection. Pre-injection of M6P-GFLG-HPMA-GFLG-ONP into fibrotic rats decreased the liver uptake of the conjugates from 60% to 13%, suggesting M6P/TGFII receptor-mediated endocytosis of the conjugates by HSCs. Almost 80% of the total liver uptake in fibrotic rats was contributed by HSCs. In conclusion, conjugation with M6P-HPMA-GFLG significantly increased TFO delivery to the HSCs and could be potentially used for treating liver fibrosis.

Keywords

triplex forming oligonucleotides; HPMA; M6P; biodistribution; hepatic stellate cells

INTRODUCTION

Chronic liver injury and inflammation of hepatocytes may lead to overproduction of type I collagen and other extracellular matrix (ECM) by hepatic stellate cells (HSCs), which are distributed throughout the hepatic lobule and serve as the principle fibrogenic cells (1). Activation of HSCs affects liver architecture and eventually liver function (2). Until now, no pharmaceutical intervention is available to treat this fibrotic disease (3). The application of most antifibrotic drugs has not been successful, partly because these drugs do not accumulate in the target liver cells or cause serious side effects elsewhere in the body. Alteration of the pharmacokinetic profiles of antifibrotic drugs by means of drug targeting represents a promising approach in the development of an effective antifibrotic drug (4).

*Address for Correspondence, Ram I Mahato, PhD, Department of Pharmaceutical Sciences, University of Tennessee Health Science Center, 19 South Manassas (Room 224), Memphis, TN 38103-3308, Tel: (901)448-6929, Fax: (901)448-2099, E-mail: E-mail: rmahato@utmem.edu, http://cop.utmem.edu/rmahato.

Direct inhibition of type I collagen synthesis by HSCs is a potential target to prevent liver fibrosis. Earlier, we developed a triplex-forming oligonucleotide (TFO), which can form a triplex with the target sequence (C1) located in the rat α1(I) collagen gene promoter and inhibit the transcription of this gene (5). Mannose-6-phosphate/insulin like growth factor II (M6P/IGFII) receptor is expressed on HSCs, and its expression is up-regulated upon activation of these cells due to acute or chronic liver injury (6). Therefore, this TFO molecule is a potential candidate for treating liver fibrosis.

Following systemic administration, oligonucleotides (ODNs) widely distribute throughout the body with higher accumulation in the liver and kidney (7–9). We determined the in vivo distribution of the TFO molecules in normal and fibrotic rats (10). Almost 45% of the injected dose was accumulated in the liver at 30 min post tail vein injection in normal rats, but only 35% of injected dose in fibrotic rats. Since the intrahepatic distribution of the TFO was non-specific, we synthesized mannose-6-phosphate-bovine serum albumin (M6P-BSA) and conjugated to TFO via a disulfide bond for its enhanced delivery to HSCs (11). Since the treatment of liver fibrosis may require repeated injections of TFO at high dose, high molecular weight globular BSA (66430 Da) may not be a suitable carrier for TFO delivery to the HSCs due to possible immune reaction. N-(2-hydroxypropyl) methacrylamide (HPMA) copolymer has shown great potential for delivery of small molecular drugs (12–14). Although HPMA has also been used for oligonucleotide delivery, no targeting ligands were used for its site-specific delivery to target cells and its biodistribution and uptake by different liver cell types was not determined after systemic administration. Even though biodistribution of oligonucleotides to the liver has been reported before (15–17), the authors did not determine oligonucleotides delivery to HSCs, which are the principal liver fibrotic cells.

In this study, we conjugated M6P to HPMA and then to TFO via GFLG linker, which is known to be cleaved by lysosomal enzymes (15). Following bioconjugation and purification, we determined i) whether TFO can be released from the conjugate after cellular uptake, ii) biodistribution of M6P-GFLG-HPMA-GFLG-^{32}P-TFO at the whole body, organ (liver) and cellular (liver cells) levels after tail vein injection into rats.

EXPERIMENTAL PROCEDURES

Materials

Poly (HPMA-co-GFLG-ONP) was purchased from Varian Inc (Amherst, MA). *p*-nitrophenyl-α-D-mannopyranoside (pnpM), phosphorous oxide chloride, palladium (10 wt % on activated carbon), papain, methylene blue, N,N'-diisopropylethylamine, Histodenz (nycodenz) and pronase were purchased from Sigma-Aldrich (St. Louis, MO). Sephadex G75 (superfine) was procured from Pharmacia Fine Chemicals AB (Uppsala, Sweden). Dialysis tubing (molecular weight cutoff of 1000 Da) was purchased from Spectrum Laboratories, Inc. (Houston, TX). BioGel P-6 DG Gel was from Bio-Rad Laboratories (Hercules, CA). [γ-^{32}P]-dATP was purchased from MP Biomedicals (Irvine, CA), and T4 polynucleotide kinase was from New England Biolabs (Beverly, MA). Soluene-350 (tissue solubilizer) and HionicFluor (scintillation fluid) were purchased from Perkin-Elmer (Boston, MA). Hydrogen peroxide (H_2O_2) was purchased from Fisher Chemical (Fair Lawn, NJ). Heparin was purchased from American Pharmaceutical Partners, Inc. (Los Angeles, CA). Ca^{2+}/Mg^{2+}–free Hank's balanced salt solution (Cellgro) was purchased from MediaTech (Washington, DC), and type IV collagenase was from Worthington Biochemical Corporation (Lakewood, NJ). Isoflurane was purchased from Baxter Pharmaceutical Products, Inc. (Deerfield, IL). TFO, which was a 25 mer antiparallel fully phosphorothioate ODN (3'-GAGGGGGGAGGAGGGAAAGGAAGGG-5') targeting rat α1 (I) collagen gene promoter, and TFO-3'-NH_2 were synthesized by Invitrogen (Carlsbad, CA). All solvents and chemicals used in this study were used as available without further purification.

Animals

Male Sprague-Dawley rats weighing 130–150 g were purchased from Harlan Co. (San Diego, CA) and were housed individually under the controlled light (12/12h) and temperature conditions and had free access to food and water.

Synthesis of p-Isothiocyanatophenyl-6-phospho-α-D-mannopyranoside

p-nitrophenyl-α-D-mannopyranoside (pnpM) (3 g, 10 mmol) was dissolved in pyridine (4 ml, 50 mmol), acetonitrile (10ml, 190 mmol), and water (0.4 ml, 22 mmol). To this solution, phosphorus oxide chloride (4 ml, 44 mmol) was added, and the mixture was stirred for 1 h at 0°C. The reaction mixture was poured onto 120 g of ice. pH was adjusted to 7.0 by slowly adding 2.5 M NaOH on ice and the neutralized solution was evaporated to dryness. The solid material was dissolved in 150 ml water. The solution was concentrated under reduced pressure at 35 °C in a rotary evaporator to a final volume of 3–4 ml. The concentrated solution was kept at 4 °C overnight for crystallization and crystals was filtered and washed with 10 ml absolute ethanol. The compound was recrystallized from a 10 ml water/100 ml ethanol mixture, redissolved in water, and lyophilized to give *p*-nitrophenyl-6-phospho-α-D-mannopyranoside (pnpM6P). pnpM6P (1 mmol) was dissolved in 20ml of a 4:1 (v/v) methanol-water mixture. To this solution, 30 mg of 10% palladium on activated carbon was added. The suspension was stirred under hydrogen (1 atm) at room temperature for two hours. After filtration, the methanolic solution was evaporated under reduced pressure at 40 °C and lyophilized to give p-aminophenyl-6-phospho-α-D-mannopyranoside (papM6P).

Synthesis of M6P-GFLG-HPMA-GFLG-TFO conjugate

The synthesis scheme of M6P-GFLG-HPMA-GFLG-TFO is shown in Figure 1. Poly(HPMA-co-MA-GFLG-ONP) (5mg, 2.25μmol of ONP) and TFO-NH_2 (0.8mg, 0.1μmol) were dissolved in anhydrous dimethyl sulfoxide (DMSO, 100μl). Then, N,N'-diisopropylethylamine (DIPEA, 3μl) was added and reacted overnight at room temperature. papM6P (3 mg, 10 μmol) was dissolved in H_2O (100μl) and dimethyl sulfoxide (DMSO) (200μl) mixture, and DIPEA (3μl) was added. Reaction was allowed to proceed for 24 h at room temperature. The reaction mixture was dialyzed against H_2O for a day, purified on a Sephadex G75 Gel column with pure water, freeze-dried, kept in −80 °C and resuspended in 0.9% saline before use.

In Vitro Characterization

The purity of intermediate and final products were monitored by reverse phase-high performance liquid chromatography (RP-HPLC), which was carried on Altech Prosphere C18 column (250mm×4.6mm×5μm) by Waters Breeze HPLC/GPC system (Waters, Milford, MA) with detection at 260nm using a gradient of 40% to 100% acetonitrile in 0.1M triethylammonium acetate (TEAA) at a flow rate of 1mL/min at room temperature. M6P-GFLG-HPMA-GFLG-^{32}P-TFO was analyzed by 20% polyacrylamide gel electrophoresis (PAGE) at 80 V for 2 h. The gels were stained with methylene blue or autoradiographed.

The molecular weight of M6P-GFLG-HPMA-GFLG-TFO was also measured by gel permeation chromatography (GPC), which was carried on Waters Ultrahydrogel 250 column (7.8×300mm) by Waters Breeze HPLC/GPC system (Waters, Milford, MA) with Waters 2414 Refractive Index detector and mobile phase containing 0.02% sodium azide (NaN_3) in HPLC water, at a flow rate of 0.5 ml/min. Polyethylene oxide (PEO) of different molecular weights (MW = 20000, 31380, 50450 and 71700 Da) was used as standards for calibration. HPMA-co-MA-ONP was used as a positive control and the molecular weight of M6P-GFLG-HPMA-GFLG-TFO was determined.

Determination of Sugar Content

Sugar content was determined by the resorcinol-sulfuric acid method.(18) Two hundred microliters of 6 mg/ml resorcinol and 1 ml of 75% sulfuric acid were added to M6P-GFLG-HPMA-GFLG-TFO solution containing 5–100 nmol of sugar in 200μl. The mixtures were vortexed and heated at 90 °C for 30 min and subsequently placed in a cold-water bath for 30 min in the dark. The optical density of the solution was measured at 430 nm. PnpM was used to generate the standard curve to calculate the number of M6P per conjugate.

In Vitro Enzymatic Dissociation and Triplex Formation of M6P-GFLG-HPMA-GFLG-^{32}P-TFO

To determine whether TFO will be dissociated from M6P-GFLG-HPMA-GFLG-TFO conjugate after cellular uptake, papain (10μM), glutathione (GSH, 250mM) and M6P-GFLG-HPMA-GFLG-^{32}P-TFO (TFO concentration 100μM) were incubated together at 37 °C in 0.1M phosphate buffer containing 1mM EDTA (PE buffer, total volume of 300μl). At 1, 2, 8 and 24h, 100μl of the sample was collected and analyzed by 20% PAGE at 80 V for 2 h, followed by autoradiography.

To determine whether the TFO released from M6P-GFLG-HPMA-GFLG-TFO can still form triplex, the target duplex DNA was prepared by equal amounts of ODNs, T1: 5'-GAG GGG GGA GGA GGG AAA GGA AGG GAA AGG-3' and T2: 5'-CCT TTC CCT TCC TTT CCC TCC TCC CCC CTC-3', being heated at 80 °C for 5 min in 0.25 M NaCl, followed by slow cooling to room temperature. Triplex formation was initiated by the mixing of 3 μL of 3× buffer [135 mM Tris-acetate, pH 7.0, 30 mM $MgCl_2$], 3.5 μL of duplex DNA (~3 μg), and 2.5 μL of the released ^{32}P-TFO (~1×10^5 cpm). The reaction mixture was incubated at 37 °C for another 24 h. Two microliters of a 50% glycerol solution containing bromophenol blue was added, and samples were directly loaded onto 15% native polyacrylamide gel, prepared in a buffer containing 50 mM Tris-acetate, pH 7.0, and 10 mM $MgCl_2$. Electrophoresis was performed at 8 V/cm at 4 °C in the buffer containing 89 mM Tris-Borate and 20 mM $MgCl_2$. The gel was autoradiographed at 4 °C overnight.

Transfection of TFO and M6P-GFLG-HPMA-GFLG-TFO

Immortalized rat hepatic stellate cells (HSC-T6) kindly provided by Dr Scott Friedman of Mount Sinai School of Medicine, New York were seeded in 6-well plates at a density of 11×10^5 cells 12 h until 50% confluence in DMEM containing 10% of FBS. The growth medium was replaced with a pre-warmed serum-free DMEM medium. TFO was mixed with pyridinium cationic liposome at 3/1 (+/−) charge ratio and then used for transfection at the dose of 5 μg TFO/well. For the conjugate, M6P-GFLG-HPMA-GFLG-TFO was dissolved in saline and applied to the cells at the dose of 5 μg TFO. Negative control wells were added the same amount M6P-GFLG-HPMA. Six hours later 10% FBS was added to each well, and then the cells were cultured for additional 72 h. Following transfection, the cell culture medium was concentrated using Microcon YM-30 columns (Millipore) to retain proteins of >30kDa. The concentrated medium was lysed using 2× Laemmli sodium dodecyl sulfate (SDS) sample buffer containing 100 mM Tris, pH 6.8, 200 mM dithiothreitol (DTT), 4% SDS, 20% glycerol and 0.2% bromophenol blue. To detect β-actin which was used as an intrinsic reference of sample loading, the cells were lysed directly with 1× Laemmli SDS sample buffer. The lysate samples were boiled at 100°C for 5min and subjected to 4% to 15% SDS-polyacrylamide (SDS-PAGE) gel electrophoresis and subsequently transferred to Immobilon polyvinylidene fluoride (PVDF) membrane (Millipore). After blocking with 5% non fat dried milk in 1× PBST containing 0.05% Tween-20 in PBS for 1h at room temperature, the membrane was incubated with goat anti-rat type I collagen and β-actin primary antibodies (Santa Cruz) for 16h at 4°C. The membranes were then incubated with horseradish peroxidase (HRP)-conjugated donkey anti-goat secondary antibody (Santa Cruz) for 1h at room temperature. Target proteins were detected by enhanced chemiluminescence (ECL, GE Healthcare).

Biodistribution of M6P-GFLG-HPMA-GFLG-^{32}P-TFO

The animal protocol was approved by the Animal Care and Use Committee (ACUC), Department of Comparative Medicine, University of Tennessee Health Science Center, Memphis, TN 38163. Male Sprague-Dawley rats weighing 130–150 g were used in this study and three rats were used for each time point. Unlabeled and M6P-GFLG-HPMA-GFLG-^{32}P-TFO were mixed in saline to give a final concentration of 1 mg/ml and specific activity of 1×10^6 cpm/ml. Rats were anesthetized by inhalation of isoflurane, and M6P-GFLG-HPMA-GFLG-^{32}P-TFO was injected via tail vein at a dose of 0.2 mg/kg body weight. At 2.5, 5, 15, 30, 60 and 90 min postinjection, 0.5 ml blood was collected by cardiac puncture in heparinized tubes, and urine was collected directly from the bladder using a 0.26 gauge needle syringe. The animals were then sacrificed and major tissues (liver, kidney, spleen, heart, and lung) were collected, washed, blotted dry, weighed, and stored at −80 °C. The radioactivity of the urine sample was counted directly after adding 10 ml of scintillation fluid. One hundred and fifty microliters of plasma and 150 mg of each tissue were incubated with 2 ml tissue solubilizer for 3 h at 55 °C and overnight at 37 °C in a shaker. Four hundred microliters of H_2O_2 was added and incubated at 55 °C for another 30 min. Ten milliliters of scintillation fluid was added to each sample and the radioactivity was counted using a liquid scintillation counter.

Determination of Pharmacokinetic Profiles

Plasma data were analyzed using *WinNonlin Professional* (version 5.2, Pharsight Corporation, Mountain View, CA). M6P-GFLG-HPMA-GFLG-^{32}P-TFO plasma concentration data versus time were fitted into a two-compartment model, where

$$\frac{dX_1}{dt} = k_{21} * X_2 - (k_{10} + k_{12}) * X_1 = \frac{dC_p}{dt} * V_1 \quad (1)$$

$$\frac{dX_2}{dt} = k_{12} * X_1 - k_{21} * X_2 = \frac{dC_t}{dt} * V_2 \quad (2)$$

where X_1 is amount of drug in the central compartment, and X_2 is the amount of the drug in the peripheral compartment. Since we assumed that elimination only occurred from the central compartment, k_{12} and k_{21} are the rate constants for efflux from the plasma to tissues and from tissues to the plasma, respectively. k_{10} is the elimination constant of central compartment. The change in the amount of radioactivity of M6P-GFLG-HPMA-GFLG-^{32}P-TFO in the plasma with time can be described as biexponential equation.

$$C_p(t) = A * e^{-\alpha * t} + B * e^{-\beta * t} \quad (3)$$

where α and β are the hybrid constants for distribution and elimination, respectively. C_p represents the plasma concentration at time t; A and B are the Y-axis intercepts, where

$$A = \frac{\text{Dose} * (\alpha - k_{21})}{V_1 * (\alpha - \beta)} \qquad B = \frac{\text{Dose} * (k_{21} - \beta)}{V_1 * (\alpha - \beta)} \quad (4)$$

The change in the amount of radioactivity in a tissue with time can be described as follows:

$$Q(t)=\frac{Dose*k_{12}}{V_2*(\alpha-\beta)}*(e^{-\alpha*t}-e^{-\beta*t}) \quad (5)$$

where Q(t) (% of dose/g) represents the amount of radioactivity in 1 g of the tissue, and $C_p(t)$ (% of dose/mL) is the plasma concentration of radioactivity.

$$\frac{dQ(t)}{dt}=k_{12}*C_p(t)-k_{21}*C_t(t) \quad (6)$$

where k_{12} (h^{-1}) and k_{21} (h^{-1}), as mentioned above, are the rate constant for efflux from the plasma to the tissue, and from the tissue to the plasma, respectively. In the present study, the efflux process can be considered negligible during the initial time points up to 90 min. Hence, equation 6 integrates to

$$K_{12}=Q(t_1)\Big/\int_0^{t_1}C_p(t)dt=C_t(t_1)/AUC_{0-t_1} \quad (7)$$

From equation 7,

$$CL_{in}=Q(t_1)\Big/\int_0^{t_1}C(t)dt=Q(t_1)/AUC_{0-t_1} \quad (8)$$

where t_1 (h) is the sampling time. C(t) (μg TFO/ml plasma) is the plasma concentration of radioactivity, CL_{in} ($ml\cdot h^{-1}\cdot g^{-1}$) is the tissue uptake rate index from the plasma to the tissue. According to equation 8, the tissue uptake rate index is calculated using the amount of radioactivity in the tissue and the area under the plasma concentration-time curve (AUC). Then, the organ clearance (CL_{org}) is expressed as follows:

$$CL_{org}=CL_{in}*W \quad (9)$$

where W (g) is the total weight of the organ. When the tissue uptake process followed nonlinear kinetics, CL_{in} values would represent an average value for the overall experimental period. Total body clearance (CL_{total}) was calculated from AUC for infinite time (AUC_∞) by the following equation:

$$CL_{total}=Dose\Big/AUC_\infty \quad (10)$$

The tissue uptake clearance and index were calculated using the values up to 90 min after injection, assuming that TFOs were fairly stable within this period.

Induction of Liver Fibrosis

Dimethylnitrosamine (DMN) induced liver fibrosis in rats has been shown to have a pathology closely resembling that of human cirrhosis. Male Sprague-Dawley rats weighing 130–150g (Harlan Co., San Diego, CA) were housed individually under controlled light (12/12 h) and temperature conditions and had free access to food and water. To induce liver fibrosis, dimethyl nitrosamine (DMN) was injected intraperitoneally into rats at a dose of 10 mg/kg of body

weight in saline. Injections were given in the afternoons of the first three consecutive days of each week for 4 weeks.

Competition in Hepatic Uptake of M6P-BSA-33P-TFO

Two minutes before the injection of M6P-GFLG-HPMA-GFLG-^{32}P-TFO at a TFO dose of 0.2 mg/kg (specific activity: 1×10^6 cpm/ml), liver fibrotic rats received 10 mg/kg of $(M6P)_{16}$-GFLG-HPMA. At 30 min postinjection, blood and other major organs were harvested as described above for radioactivity measurement.

Isolated Rat Liver Perfusion

To determine the effect of M6P on the hepatic uptake of TFOs by hepatocytes, HSCs, Kupffer and endothelial cells, the livers of normal and fibrotic rats were perfused in situ after intravenous administration of M6P-GFLG-HPMA-GFLG-^{32}P-TFO, HPMA-GFLG-^{32}P-TFO or ^{32}P-TFO at the dose of 0.2 mg of TFO/kg body weight. At 30 min post-administration, rats (200–250g) were anesthetized by inhalation of isoflurane, 100U heparin was injected via the tail vein, the abdomen was opened, and the portal vein was cannulated with PE-60 polyethylene tube. The liver was first perfused with 2 mL of diluted heparin solution at 20 units/mL to avoid blood clogs in the liver. The liver was pre-perfused in situ with 200 ml of Ca^{2+}/Mg^{2+}-free Hank's balanced salt solution at a flow rate of 15 ml/min and was then perfused with Hank's balanced salt solution containing 0.05% type IV collagenase and 0.1% pronase for additional 250 ml at a flow rate of 10 ml/min. All the perfusion solutions were incubated at 37 °C. After perfusion, different liver cell types were separated and radioactivity was measured as described by Cheng et al (10). The contributions of various cell types to the total liver accumulation were calculated as the percentage of total hepatic uptake.

Statistical Analysis

Data were expressed as the mean ± standard deviation (SD). The difference between any two groups was determined by ANOVA. $p< 0.05$ was considered statistically significant.

RESULTS

Synthesis and *in vitro* Characterization of M6P-GFLG-HPMA-GFLG-^{32}P-TFO

The synthesis scheme of M6P-GFLG-HPMA-GFLG-TFO is shown in Figure 1. *p*-nitrophenyl-α-D-mannopyranoside (pnpM) was phosphorylated to give *p*-nitrophenyl 6-phospho-α-D-mannopyranoside (pnpM6P). This intermediate product was characterized by electron spray ionization-mass spectrum (ES-MS) as described before (11) (data not shown). RP-HPLC was used to monitor the purity of the intermediate and final products. From the RP-HPLC chromatograms of M6P, TFO, HPMA and M6P-GFLG-HPMA-GFLG-TFO (Figure 2), almost all free M6P and TFOs were removed from the conjugate after purification. M6P-GFLG-HPMA-GFLG- TFO was separated from free TFO using G75 column. As shown in Figure 2, M6P-GFLG-HPMA-GFLG-^{32}P-TFO conjugate was eluted earlier than ^{32}P-TFO. PAGE analysis of M6P-GFLG-HPMA-GFLG-^{32}P-TFO was also confirmed successful conjugation and purity of the conjugate. As shown in Figure 3, unlike free TFO, there was no band shift for the conjugate. We also measured the molecular weight of M6P-GFLG-HPMA-GFLG-TFO by gel permeation chromatography (GPC) and determined molecular weight was 51418 Da, which matched well with the calculated molecular weight by calculation of 51362 Da. Although poly(HPMA-co-GFLG-ONP) contains 8.33 mole % of ONP, the average number of M6P per conjugate was determined to be 14.67.

In Vitro Enzymatic Dissociation and Triplex Formation of M6P-GFLG-HPMA-GFLG-^{32}P-TFO

To determine whether TFO can be dissociated from M6P-GFLG-HPMA-GFLG-^{32}P-TFO endocytosis in the lysosome, the radioactivity was measured after polyacrylamide gel electrophoresis and autoradiography at 1, 2, 8 and 24 h post-incubation of the conjugate with papain at 37 °C (19). The band of the conjugate gradually disappeared along the incubation time (Figure 4). In contrast, this conjugate resulted in no band shift in the absence of papain.

GFLG linker is expected to be stable in the bloodstream but cleaved inside the cells by enzymatic dissociation by lysosomal enzymes (20). The release from the M6P-GFLG-HPMA-GFLG-TFO conjugate will enable TFO to traffic to the nucleus for triplex formation with genomic DNA. There should be no adverse effect on triplex formation due to this conjugation and cleavage. The M6P-GFLG-HPMA-GFLG-TFO conjugate was treated with papain and incubated with the target duplex DNA for another 24 h, and the sample was then applied on a 15% native polyacrylamide gel at 4 °C. Following electrophoresis, the gel was autoradiographed at 4 °C overnight. As shown in Figure 5, there was triplex formation observed with target duplex DNA not only for free TFO (lane 2) but also for released TFO (lane 6), which was at a molar ratio of 200 between duplex DNA and TFO.

Inhibition of Collagen Type I Gene Expression by M6P-GFLG-HPMA-GFLG-TFO

To confirm that TFO conjugation to M6P-HPMA does not adversely affect its ability to inhibit the transcription of type I collagen, we transfected HSC-T6 cells with TFO and M6P-GFLG-HPMA-GFLG-TFO. Compared to the control cells treated with M6P-HPMA (lane 1), type I collagen gene expression by the cells treated with M6P-GFLG-HPMA-GFLG-TFO (lane 2) decreased as efficiently as that by the cells treated with the TFO (lane 3) (Figure 6). Since the molecular weight of collagen type 1 precursor is 130–140 kDa and that of mature collage type 1 is 70–90 Da, there were 2 bands for collagen, which is in good agreement with the supplier's Western blot analysis (right figure).

Biodistribution of M6P-GFLG-HPMA-GFLG-TFO

Following synthesis and purification of M6P-GFLG-HPMA-GFLG-^{32}P-TFO, we determined the biodistribution of this conjugate at 2.5, 5, 15, 30, 60 and 90 min post injection into the rat tail vein. Figure 7 shows the time course of radioactivity in the plasma, urine, liver, kidney, lung, and heart. Conjugation with M6P-GFLG-HPMA-GFLG-ONP significantly increased the accumulation of ^{32}P-TFO in the liver, as compared to our previously reported biodistribution data of free ^{32}P-TFO (10). Almost 70% of the conjugate accumulated in the liver at 30 min postinjection and 60% at 60 min postinjection (Fig. 7), however, only 40% of free ^{32}P-TFO was in the liver at 30 min (10). Figure 8 shows the tissue concentration of M6P-GFLG-HPMA-GFLG-^{32}P-TFO in the plasma (μg/ml) and tissues (μg/g) after tail vein injection into rats. The conjugation with M6P-GFLG-HPMA-GFLG-ONP significantly increased the accumulation of radioactivity in the liver and was the highest at 30 min post-injection. The conjugate concentration was high not only in the liver, but also in the spleen and kidney. However, radioactivity in the kidney rapidly decreased with time. We also included the tissue accumulation data of ^{32}P-TFO at 30 min post-injection for comparison.

We also calculated the pharmacokinetic profiles using two-compartment model by plotting plasma concentration versus time, analyzing data using WinNonlin professional software. As shown in Figure 9, there was good fit between observed and predicted results. Plasma elimination of M6P-GFLG-HPMA-GFLG-^{32}P-TFO was biphasic with a distribution half-life ($T_{1/2\alpha}$) of 12.37 min and elimination half-life ($T_{1/2\beta}$) of 2886.48 min. Figure 9 also summarizes the pharmacokinetic parameters such as AUC, V_d and CL. Consistent with the rapid clearance (0.059 ml/min), M6P-GFLG-HPMA-GFLG-^{32}P-TFO had a large V_d of 231.33 ml, Table 1 summarizes the AUC, tissue uptake rate index, and organ clearance for representative organs

at 90 min after systemic administration of ^{32}P-TFO and M6P-GFLG-HPMA-GFLG-^{32}P-TFO in rats. The liver uptake rate indices and clearance of the conjugate were significantly higher than those of ^{32}P-TFO: 2176±58 versus 376±38 $\mu l h^{-1} g^{-1}$ and 11531±308 versus 2218±206 μl/h, respectively. The tissue uptake rate indices and organ clearances of heart, kidney, and lung were significantly higher than those of ^{32}P-TFO, possibly due to increase in vivo stability of TFO upon conjugation with M6P-GFLG-HPMA-GFLG-ONP.

Effect of Fibrosis on Biodistribution

We recently reported significant decrease in the hepatic uptake of ^{33}P-TFO when injected into fibrotic rats (10). To make sure that there is no decrease in the hepatic uptake of M6P-GFLG-HPMA-GFLG-^{32}P-TFO, we determined the biodistribution of this conjugate at 30 min post injection in fibrotic rats. To exclude the possibility that HPMA, the backbone, is not involved in the specific uptake of the TFO, we also determined the biodistribution of HPMA-GFLG-^{33}P-TFO at 30 min post-injection. There was no decrease in the hepatic uptake of M6P-GFLG-HPMA-GFLG-^{32}P-TFO in fibrotic rats (Figure 10). As expected, HPMA-GFLG-^{33}P-TFO accumulation in the liver was much less than that of M6P-GFLG-HPMA-GFLG-^{32}P-TFO and decreased when fibrotic rats were used (Figure 10). This may be due to the fact that M6P/IGFII receptors are up-regulated during fibrosis (21), which should increase the uptake by HSCs via receptor-mediated endocytosis and cancel out any adverse effect created by decrease in sinusoidal gap.

Competition in Hepatic Uptake

To determine whether the hepatic uptake of M6P-GFLG-HPMA-GFLG-^{32}P-TFO is mediated by M6P/IGFII receptor mediated endocytosis, we preinjected excess amount of $(M6P)_{16}$-GFLG-HPMA followed by injection of the conjugate in fibrotic rats. This resulted in a significant decrease in the hepatic uptake of the conjugate in fibrotic rats (Figure 11), possibly due to M6P/IGFII receptor mediated endocytosis of the conjugates.

Hepatic Cellular Localization

To determine the uptake of M6P-GFLG-HPMA-GFLG-^{32}P-TFO by different liver cell types, the livers of normal and fibrotic rats were perfused at 30 min post tail vein injection, and hepatocytes, HSCs, Kupffers and endothelial cells were isolated for determining the amount of radioactivity in these cells. As shown in Figure 12, HSCs were the major site for the uptake of this conjugate. Furthermore, the uptake of M6P-GFLG-HPMA-GFLG-^{32}P-TFO by HSCs was significantly higher compared to free ^{32}P-TFO. Although there was no significant decrease in the overall hepatic recovery of M6P-GFLG-HPMA-GFLG-^{32}P-TFO, uptake by the HSCs of DMN-induced liver fibrotic rats was much higher than that of normal rats (79.63±2.56% versus 51.55±2.02%) (Figure 12). We also perfused the livers of both normal and fibrotic rats at 30 min post-injection of HPMA-GFLG-^{32}P-TFO and determined the intrahepatic distribution of the TFO by different liver cells. As can be seen in Figure 12, the conjugation of ^{32}P-TFO with GFLG-HPMA did not significantly increase the TFO uptake by HSCs of both normal and fibrotic rats, suggesting the HPMA backbone is not involved in the specific uptake of the TFO.

DISCUSSION

Excessive production of extracellular matrix (ECM), primarily type I collagen, by activated HSCs is known to be one of the major causes of liver fibrosis (1). The entire region spanning from −140 to −200 of α1(I) collagen gene promoter exist as a symmetric polypurine-polypyrimidine tract in which the polypyrimidine sequence at −141 to −170 is called C1 region present on the non-coding strand, whereas the adjacent polypurine sequence from −171 to −200 is called C2 region located on the coding strand. The cis-acting element is the C1 and C2

regions, playing an important role in collagen transcription (22). We have previously demonstrated that TFOs could form triplex in this region and inhibit the activity of α1(I) collagen promoter in vitro (5,23). In addition, TFOs have been shown to partly reverse fibrosis in a dimethylnitrosamine (DMN) induced liver fibrosis rats, indicating the therapeutic potential of these TFOs (10).

M6P is a ligand for M6P/IGF II receptor, which is up-regulated in activated HSCs during liver fibrosis, enabling selective accumulation of M6P-conjugated carrier or drug molecules (24). M6P conjugation to albumin increased the uptake of M6P-BSA by HSCs in liver fibrotic rats. (25) Conjugation of M6P to virus recombinant interleukein-10 (vIL-10) significantly increased the hepatic uptake of vIL-10 by the liver.

To avoid the use of polycations, Rajur et al. conjugated ODNs to asialoorosomucoid via disulfide bond (26). However, this strategy is not suitable for the TFO, since direct conjugation of molecules to the TFOs often disrupts the triplex-forming ability of the TFOs, which is essential for transcription inhibition. Furthermore, liver fibrosis results in the loss of sinusoidal fenestrae, suggesting that particulate delivery systems may not be good for TFO delivery to the HSCs.

To avoid any non-specific ionic interaction and the large particle size, we recently conjugated TFO to M6P-BSA via a disulfide bond and demonstrated enhanced uptake by the HSCs after systemic administration of M6P-BSA-TFO into normal and fibrotic rats (27). However, repeated administration of this conjugate is likely to cause immune reaction due to BSA and thus we synthesized M6P-GFLG-HPMA-GFLG-ONP and conjugated to TFO, where GFLG is a lysosomally degradable tetrapeptide, and thus will facilitate lysosomal release of TFO and its escape to the cytoplasm after cellular uptake. Following synthesis and characterization using RP-HPLC and GPC, we determined whether TFO could be dissociated from the conjugate by incubating M6P-GFLG-HPMA-GFLG-TFO with papain and TFO release was monitored. As shown in Figure 4, free TFO release concentration increased with incubation time with papain, which is consistent with the literature (20). Papain is a cysteine protease hydrolase enzyme and belongs to the same family as cathepsin B, which is the most important enzyme in the lysosomes to cleave GFLG spacer (17,19,20).

To make sure the TFO released from the conjugate can form a triplex to the target duplex DNA, we incubated M6P-GFLG-HPMA-GFLG-TFO with papain for 24 h and then used the released TFO to form triplex with the target duplex DNA. As can be seen in Figure 5, the TFO released from the conjugate formed triplex with duplex DNA.

To confirm that TFO conjugation to M6P-GFLG-HPMA does not adversely affect its ability to inhibit the transcription of type I collagen, we transfected HSC-T6 cells with M6P-GFLG-HPMA-GFLG-TFO. Compared to the control cells treated with M6P-HPMA, type I collagen gene expression by the cells treated with M6P-GFLG-HPMA-GFLG-TFO decreased as efficiently as that by the cells treated with the TFO (Figure 6).

Conjugation of TFO to M6P-GFLG-HPMA-GFLG-ONP significantly increased TFO delivery to the liver from 47% for ^{32}P-TFO to 70% for M6P-GFLG-HPMA-GFLG-^{32}P-TFO at 30 min post injection. To determine whether the hepatic uptake of M6P-GFLG-HPMA-GFLG-^{32}P-TFO is mediated by M6P/IGF II receptor mediated endocytosis, we preinjected rats with excess amount of M6P-GFLG-HPMA-GFLG-ONP. This resulted in a significantly decrease in the hepatic accumulation of this conjugate in fibrotic rats (Figure 11). This confirmed the receptor-mediated uptake of this conjugate, since M6P/TGF II receptor is up-regulated in liver fibrotic rats, the hepatic accumulation was almost completely inhibiting by saturating this receptor. Rachmawati et al also demonstrated almost 50% inhibition in the hepatic uptake of M6P-IL-10 conjugates in fibrotic rats (28).

To determine the hepatic cellular localization, the liver was perfused at 30 min post-injection of M6P-GFLG-HPMA-GFLG-^{32}P-TFO, HPMA-GFLG-^{32}P-TFO or ^{32}P-TFO and different liver cells were separated by fractionation on the Histodenz gradient. As shown in Figure 12, almost 80% of the total liver uptake was contributed by HSCs cells of fibrotic rats, but only 55% by HSCs of normal rats. The percentage of uptake by hepatocytes was relatively low in both normal and fibrotic rats. However, the conjugation of TFO with GFLG-HPMA did not significantly increase the TFO uptake by HSCs of both normal and fibrotic rats (Figure 12); suggesting the HPMA backbone is not involved in the specific uptake of the TFO.

In conclusion, conjugate with M6P-GFLG-HPMA-GFLG-ONP significantly enhance the uptake of the TFO by HSCs and thus this conjugate may be suitable for inhibiting α1 (I) collagen gene expression by HSCs and potentially treat liver fibrosis.

ACKNOWLEDGEMENT

This work was supported by a grant EB003922 from the National Institutes of Health. The authors thank for Lin Zhu for help in animal experiments.

REFERENCES

1. Ye Z, Houssein HS, Mahato RI. Bioconjugation of oligonucleotides for treating liver fibrosis. Oligonucleotides 2007;17:349–404. [PubMed: 18154454]
2. Friedman SL. Molecular regulation of hepatic fibrosis, an integrated cellular response to tissue injury. J Biol Chem 2000;275:2247–2250. [PubMed: 10644669]
3. Pinzani M, Rombouts K, Colagrande S. Fibrosis in chronic liver diseases: diagnosis and management. J Hepatol 2005;42 Suppl:S22–S36. [PubMed: 15777570]
4. Hagens WI, Mattos A, Greupink R, de Jager-Krikken A, Reker-Smit C, van Loenen-Weemaes A, Gouw IA, Poelstra K, Beljaars L. Targeting 15d-prostaglandin J2 to hepatic stellate cells: two options evaluated. Pharm Res 2007;24:566–574. [PubMed: 17245650]
5. Ye Z, Guntaka RV, Mahato RI. Sequence-specific triple helix formation with genomic DNA. Biochemistry 2007;46:11240–11252. [PubMed: 17845009]
6. Cheng K, Mahato RI. Gene modulation for treating liver fibrosis. Crit Rev Ther Drug Carrier Syst 2007;24:93–146. [PubMed: 17725523]
7. Sawai K, Mahato RI, Oka Y, Takakura Y, Hashida M. Disposition of oligonucleotides in isolated perfused rat kidney: involvement of scavenger receptors in their renal uptake. J Pharmacol Exp Ther 1996;279:284–290. [PubMed: 8859005]
8. Agrawal S, Temsamani J, Tang JY. Pharmacokinetics, biodistribution, and stability of oligodeoxynucleotide phosphorothioates in mice. Proc Natl Acad Sci U S A 1991;88:7595–7599. [PubMed: 1881900]
9. Takakura Y, Mahato RI, Yoshida M, Kanamaru T, Hashida M. Uptake characteristics of oligonucleotides in the isolated rat liver perfusion system. Antisense Nucleic Acid Drug Dev 1996;6:177–183. [PubMed: 8915502]
10. Cheng K, Ye Z, Guntaka RV, Mahato RI. Biodistribution and hepatic uptake of triplex-forming oligonucleotides against type alpha1(I) collagen gene promoter in normal and fibrotic rats. Mol Pharm 2005;2:206–217. [PubMed: 15934781]
11. Ye Z, Cheng K, Guntaka RV, Mahato RI. Targeted delivery of a triplex-forming oligonucleotide to hepatic stellate cells. Biochemistry 2005;44:4466–4476. [PubMed: 15766277]
12. Kopecek J, Kopeckova P, Minko T, Lu Z. HPMA copolymer-anticancer drug conjugates: design, activity, and mechanism of action. Eur J Pharm Biopharm 2000;50:61–81. [PubMed: 10840193]
13. Gao SQ, Lu ZR, Petri B, Kopeckova P, Kopecek J. Colon-specific 9-aminocamptothecin-HPMA copolymer conjugates containing a 1,6-elimination spacer. J Control Release 2006;110:323–331. [PubMed: 16290118]
14. Sirova M, Strohalm J, Subr V, Plocova D, Rossmann P, Mrkvan T, Ulbrich K, Rihova B. Treatment with HPMA copolymer-based doxorubicin conjugate containing human immunoglobulin induces

long-lasting systemic anti-tumour immunity in mice. Cancer Immunol Immunother 2007;56:35–47. [PubMed: 16636810]

15. Jensen KD, Kopeckova P, Kopecek J. Antisense oligonucleotides delivered to the lysosome escape and actively inhibit the hepatitis B virus. Bioconjug Chem 2002;13:975–984. [PubMed: 12236779]
16. Jensen KD, Nori A, Tijerina M, Kopeckova P, Kopecek J. Cytoplasmic delivery and nuclear targeting of synthetic macromolecules. J Control Release 2003;87:89–105. [PubMed: 12618026]
17. Wang L, Kristensen J, Ruffner DE. Delivery of antisense oligonucleotides using HPMA polymer: synthesis of A thiol polymer and its conjugation to water-soluble molecules. Bioconjug Chem 1998;9:749–757. [PubMed: 9815169]
18. Monsigny M, Petit C, Roche AC. Colorimetric determination of neutral sugars by a resorcinol sulfuric acid micromethod. Anal Biochem 1988;175:525–530. [PubMed: 3239778]
19. Lu ZR, Gao SQ, Kopeckova P, Kopecek J. Modification of cyclosporin A and conjugation of its derivative to HPMA copolymers. Bioconjug Chem 2001;12:129–133. [PubMed: 11170375]
20. Ding H, Kopeckova P, Kopecek J. Self-association properties of HPMA copolymers containing an amphipathic heptapeptide. J Drug Target 2007;15:465–474. [PubMed: 17671893]
21. De Bleser PJ, Scott CD, Niki T, Xu G, Wisse E, Geerts A. Insulinlike growth factor II/mannose 6-phosphate-receptor expression in liver and serum during acute CCl4 intoxication in the rat. Hepatology 1996;23:1530–1537. [PubMed: 8675174]
22. Joseph J, Kandala JC, Veerapanane D, Weber KT, Guntaka RV. Antiparallel polypurine phosphorothioate oligonucleotides form stable triplexes with the rat alpha1(I) collagen gene promoter and inhibit transcription in cultured rat fibroblasts. Nucleic Acids Res 1997;25:2182–2188. [PubMed: 9153319]
23. Nakanishi M, Weber KT, Guntaka RV. Triple helix formation with the promoter of human alpha1(I) procollagen gene by an antiparallel triplex-forming oligodeoxyribonucleotide. Nucleic Acids Res 1998;26:5218–5222. [PubMed: 9801322]
24. Beljaars L, Olinga P, Molema G, de Bleser P, Geerts A, Groothuis GM, Meijer DK, Poelstra K. Characteristics of the hepatic stellate cell-selective carrier mannose 6-phosphate modified albumin (M6P(28)-HSA). Liver 2001;21:320–328. [PubMed: 11589768]
25. Beljaars L, Molema G, Weert B, Bonnema H, Olinga P, Groothuis GM, Meijer DK, Poelstra K. Albumin modified with mannose 6-phosphate: A potential carrier for selective delivery of antifibrotic drugs to rat and human hepatic stellate cells. Hepatology 1999;29:1486–1493. [PubMed: 10216133]
26. Rajur SB, Roth CM, Morgan JR, Yarmush ML. Covalent protein-oligonucleotide conjugates for efficient delivery of antisense molecules. Bioconjug Chem 1997;8:935–940. [PubMed: 9404669]
27. Ye Z, Cheng K, Guntaka RV, Mahato RI. Receptor-mediated hepatic uptake of M6P-BSA-conjugated triplex-forming oligonucleotides in rats. Bioconjug Chem 2006;17:823–830. [PubMed: 16704223]
28. Rachmawati H, Reker-Smit C, Lub-de Hooge MN, van Loenen-Weemaes A, Poelstra K, Beljaars L. Chemical modification of interleukin-10 with mannose 6-phosphate groups yields a liver-selective cytokine. Drug Metab Dispos 2007;35:814–821. [PubMed: 17312017]

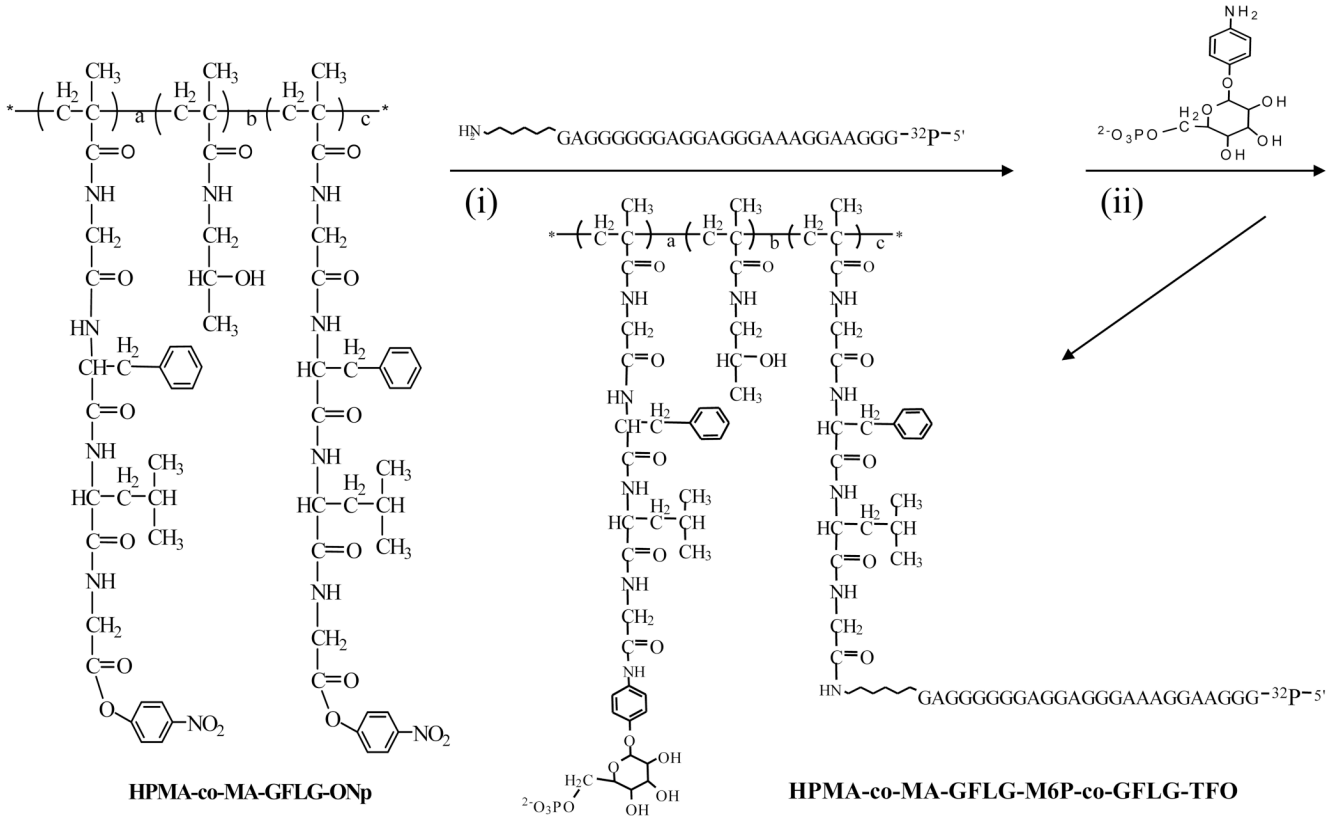

Figure 1.
Synthesis scheme of M6P-GFLG-HPMA-GFLG-TFO.

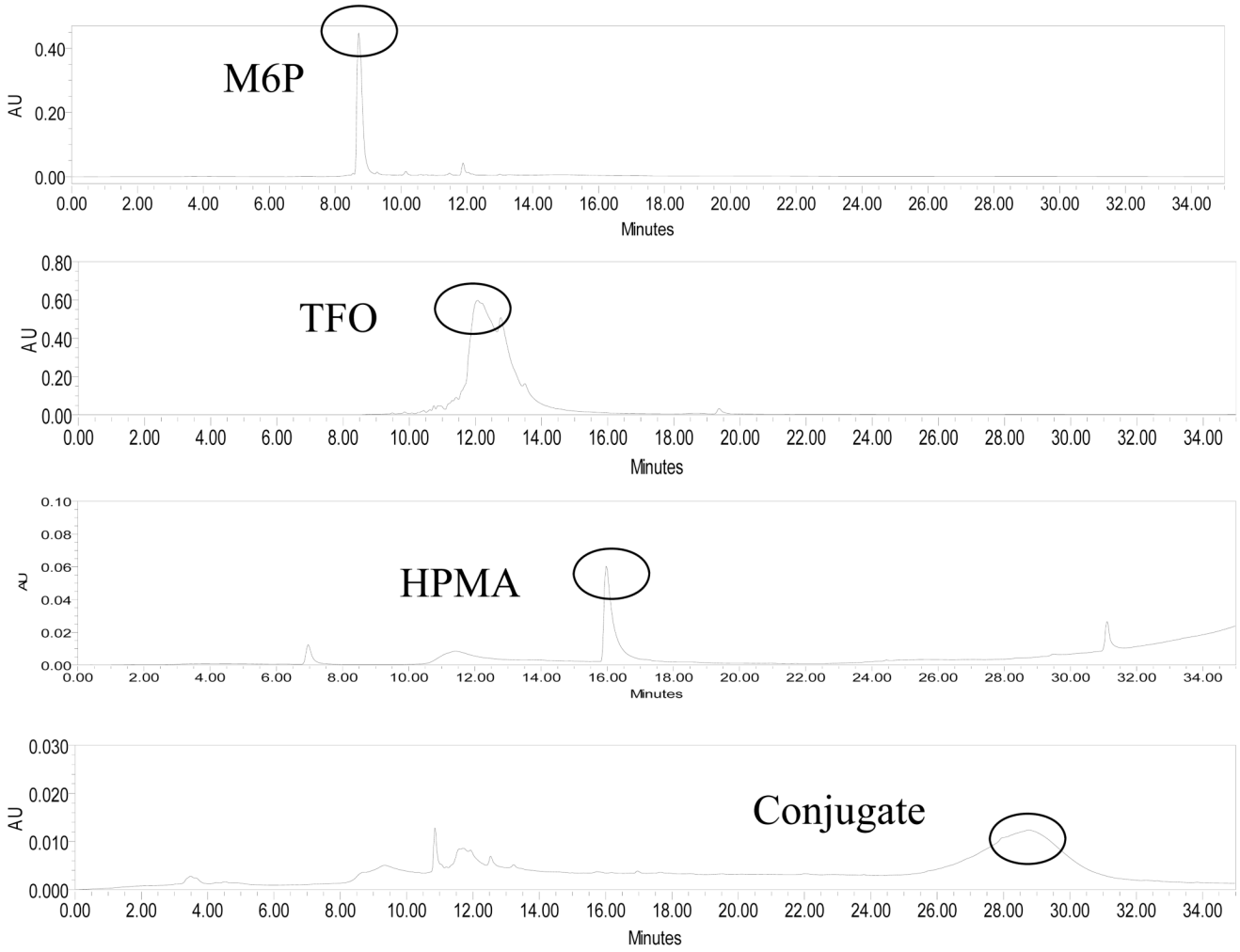

Figure 2.
HPLC chromatography of M6P-GFLG-HPMA-GFLG-TFO conjugate. There is a new peak for conjugate different from the reactants, such as M6P, poly(HPMA-co-GFLG-ONP) and TFO.

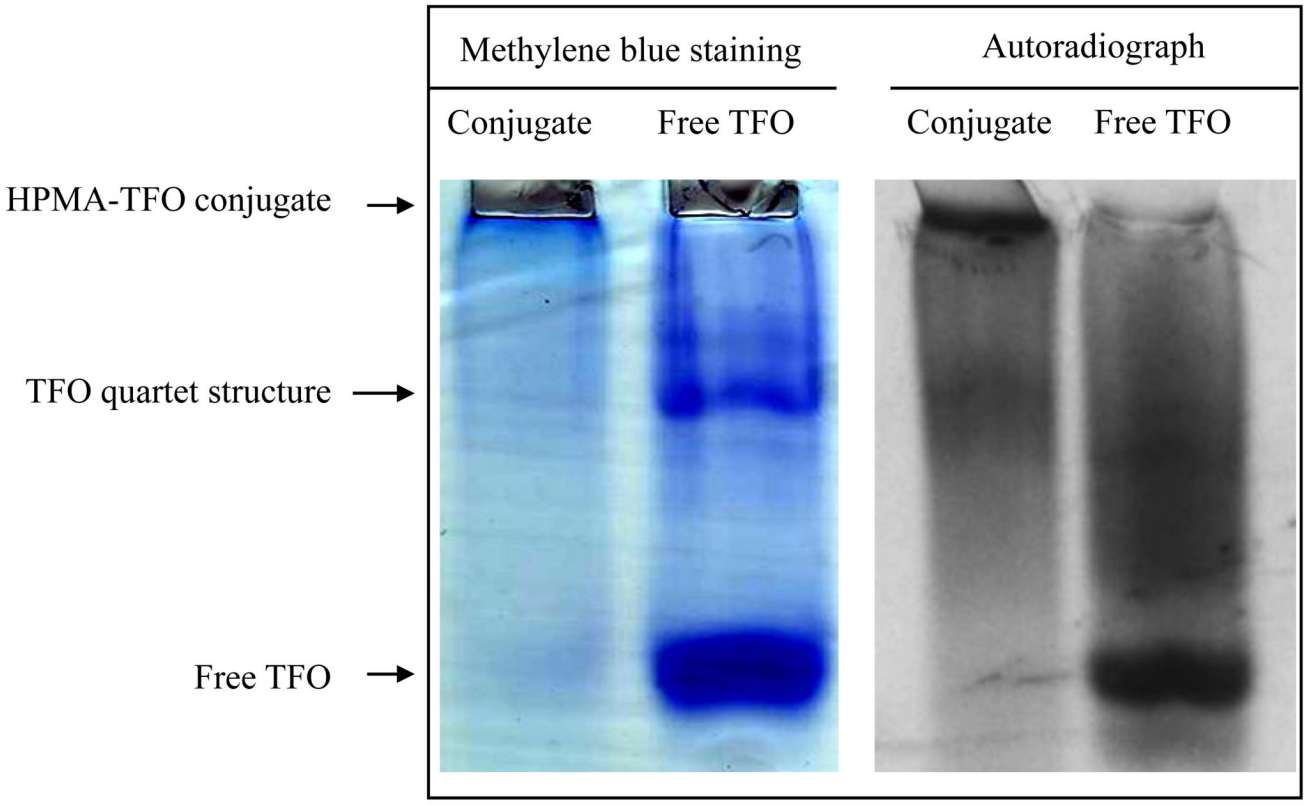

Figure 3.
Polyacrylamide gel electrophoresis (PAGE) of M6P-GFLG-HPMA-GFLG-TFO. A) methylene blue staining. B) autoradiography. There was no band shift for the conjugate.

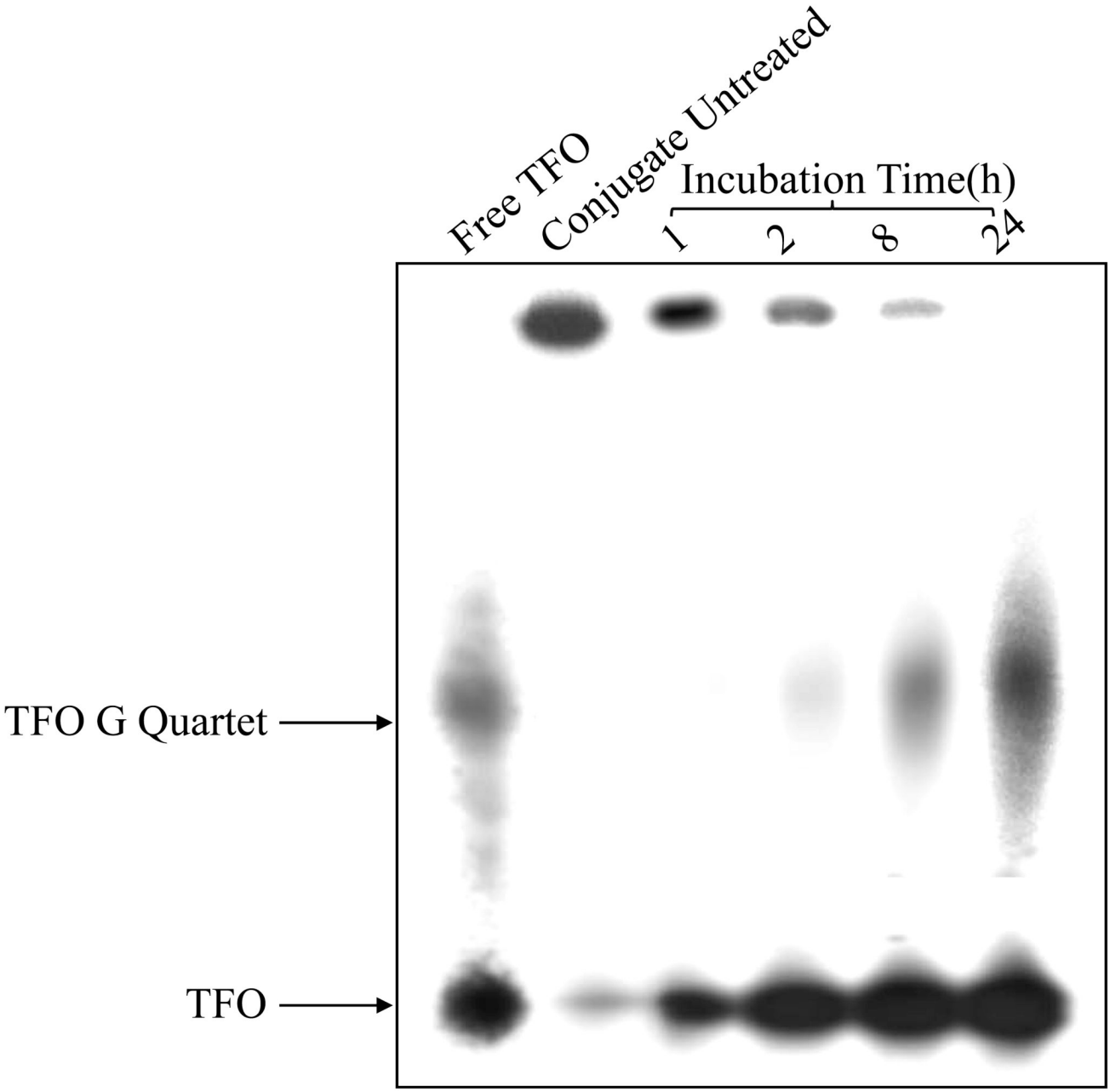

Figure 4.
TFO dissociation from M6P-GFLG-HPMA-GFLG-TFO by papain. The conjugate was treated with papain for 1h, 2h, 8h, 24h followed by polyacrylamide gel electrophoresis (PAGE) and autoradiography. The conjugate not treated with papain was used as a control.

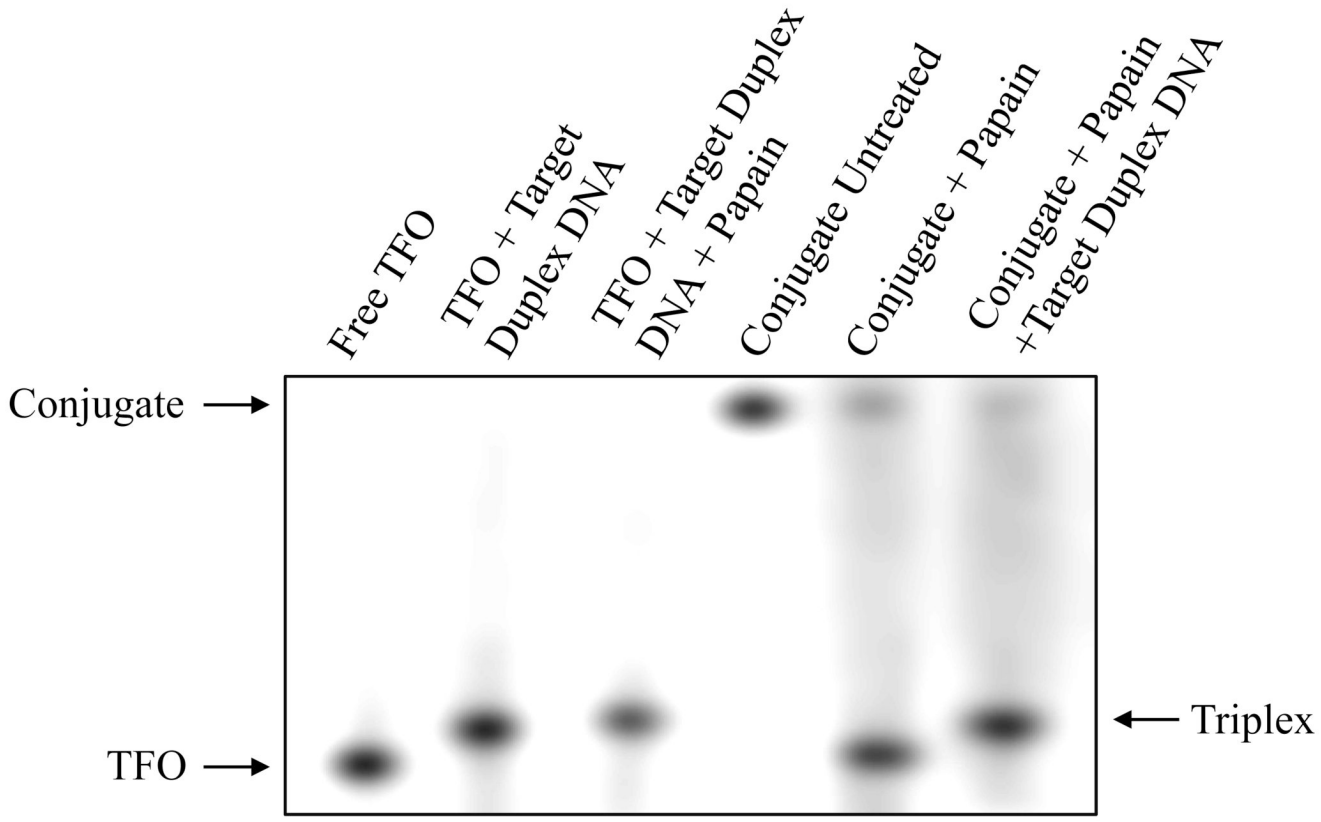

Figure 5.

Triplex formation with target duplex DNA after release from M6P-GFLG-HPMA-GFLG-^{32}P-TFO conjugate. Samples were applied on 15% native PAGE at 4 °C in 89 mM Tris-borate buffer, containing $MgCl_2$ (20 mM) for 4 h. Lane 1: ^{32}P-TFO; lane 2: duplex DNA/^{32}P-TFO (200:1) incubated for 24 h; lane 3: Duplex DNA/^{32}P-TFO (200:1) and papain incubated for 24 h; lane 4: M6P-GFLG-HPMA-GFLG-^{32}P-TFO; lane 5: M6P-GFLG-HPMA-GFLG-^{32}P-TFO incubated with papain for 24 h at 37 °C; and lane 6: duplex DNA/M6P-GFLG-HPMA-GFLG-^{32}P-TFO (200:1) incubated for 24 h at 37 °C with papain.

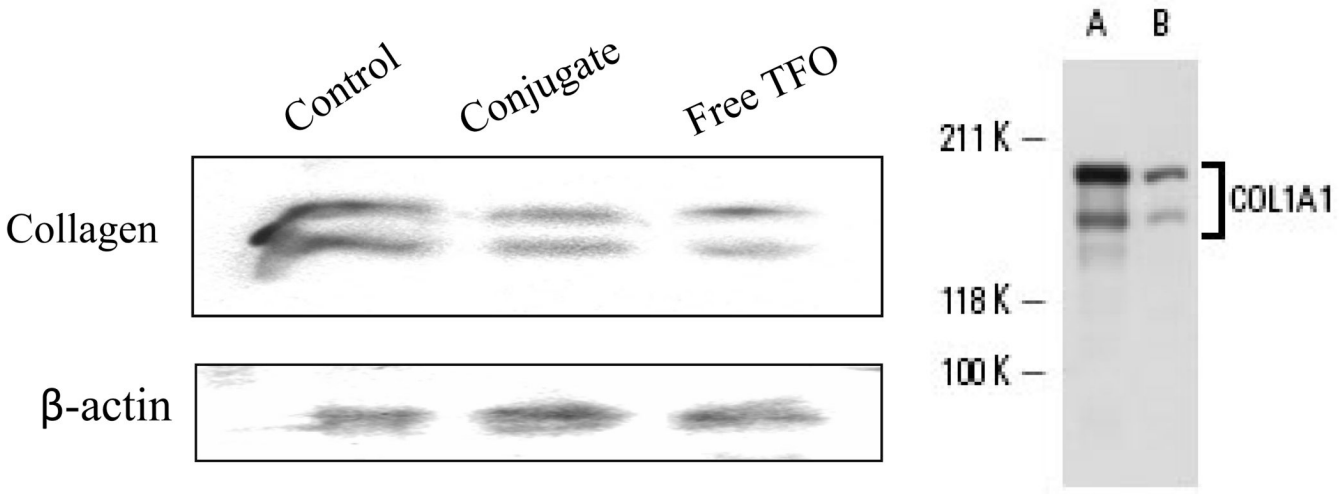

Figure 6.

Inhibition of collagen gene expression. Transfection of HSC-T6 cells with TFO (lane 3) and M6P-GFLG-HPMA-GFLG-TFO (lane 2) inhibited collagen gene expression compared to the control group (lane 1). Western blot analysis of collagen primary antibody provided Santa Cruz was also shown in the right figure.

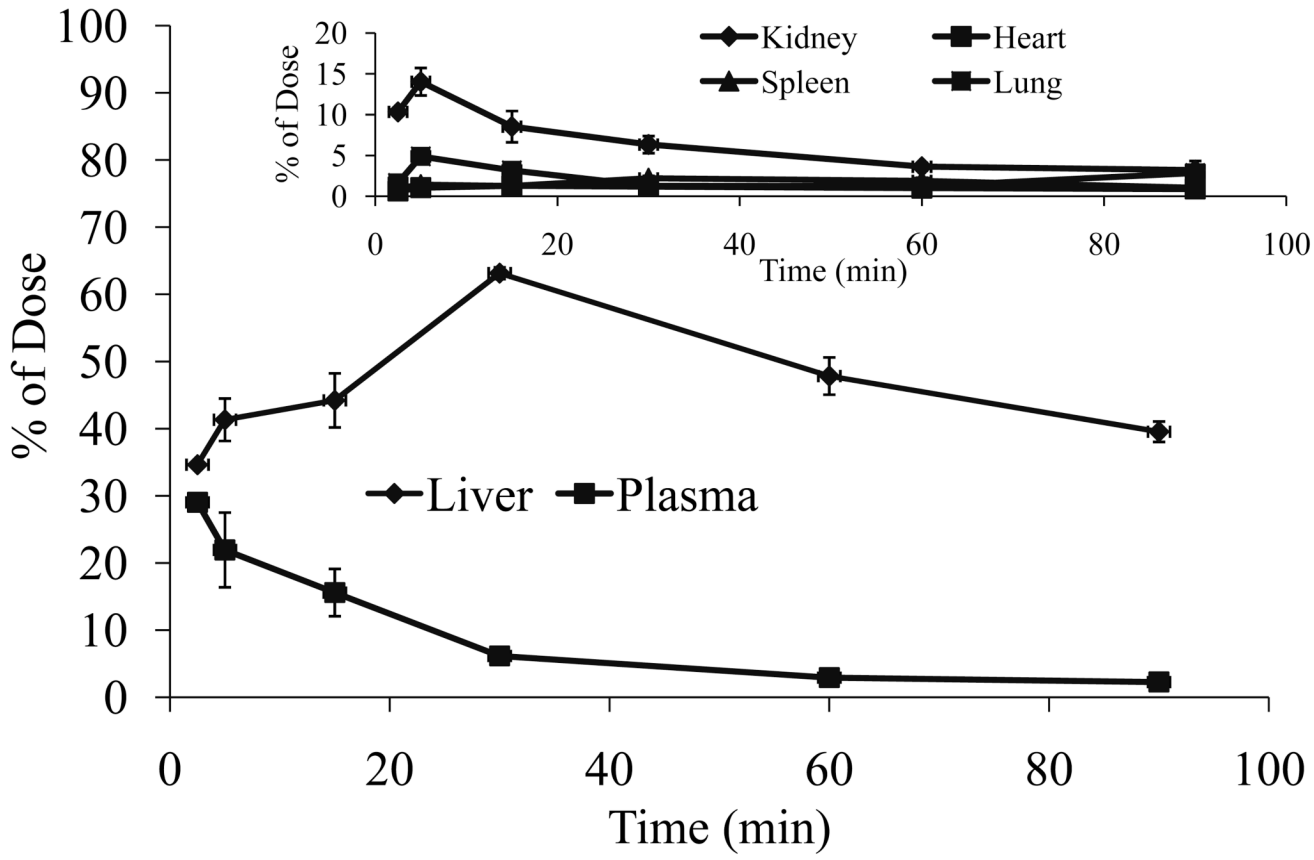

Figure 7.
Biodistribution of M6P-GFLG-HPMA-GFLG-^{32}P-TFO and free ^{32}P-TFO after tail vein injection into rats at a dose of 0.2 mg TFO/kg of body weight.

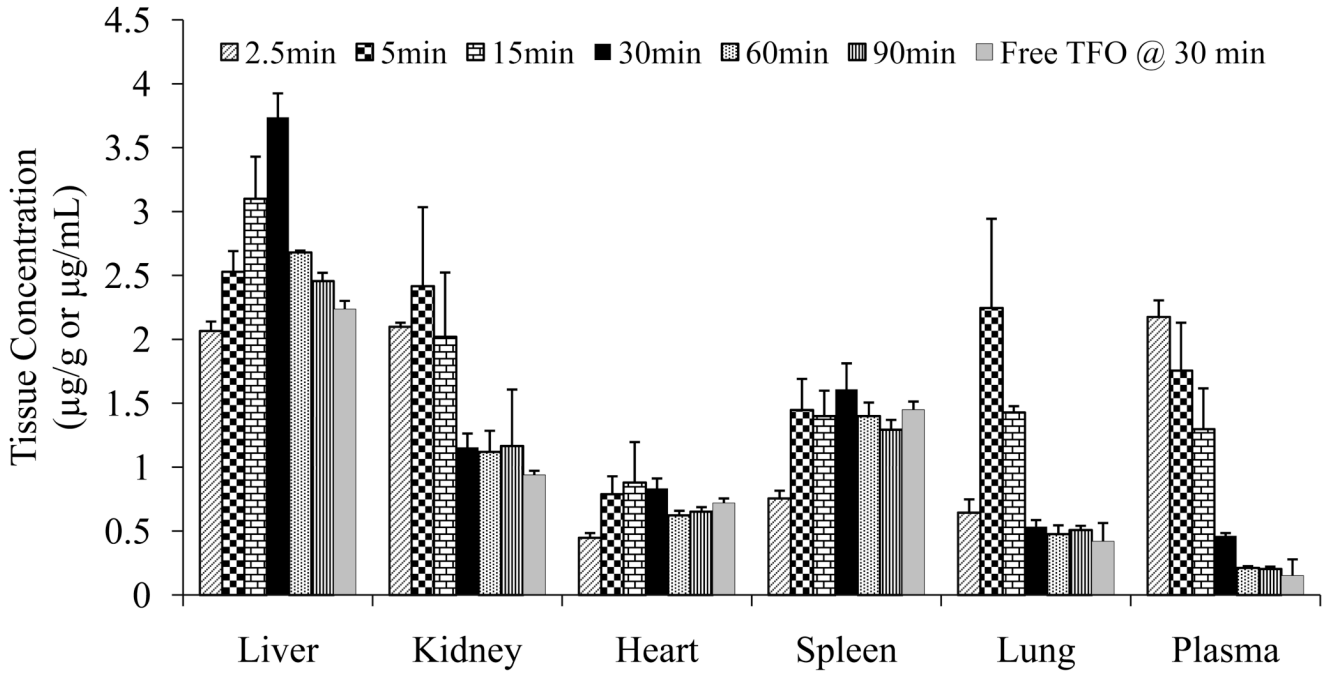

Figure 8.

Concentration time profiles of radioactivity in different organs and the plasma after tail vein injection of M6P-GFLG-HPMA-GFLG-^{32}P-TFO and free ^{32}P-TFO into rats at a dose of 0.2 mg TFO/kg of body weight.

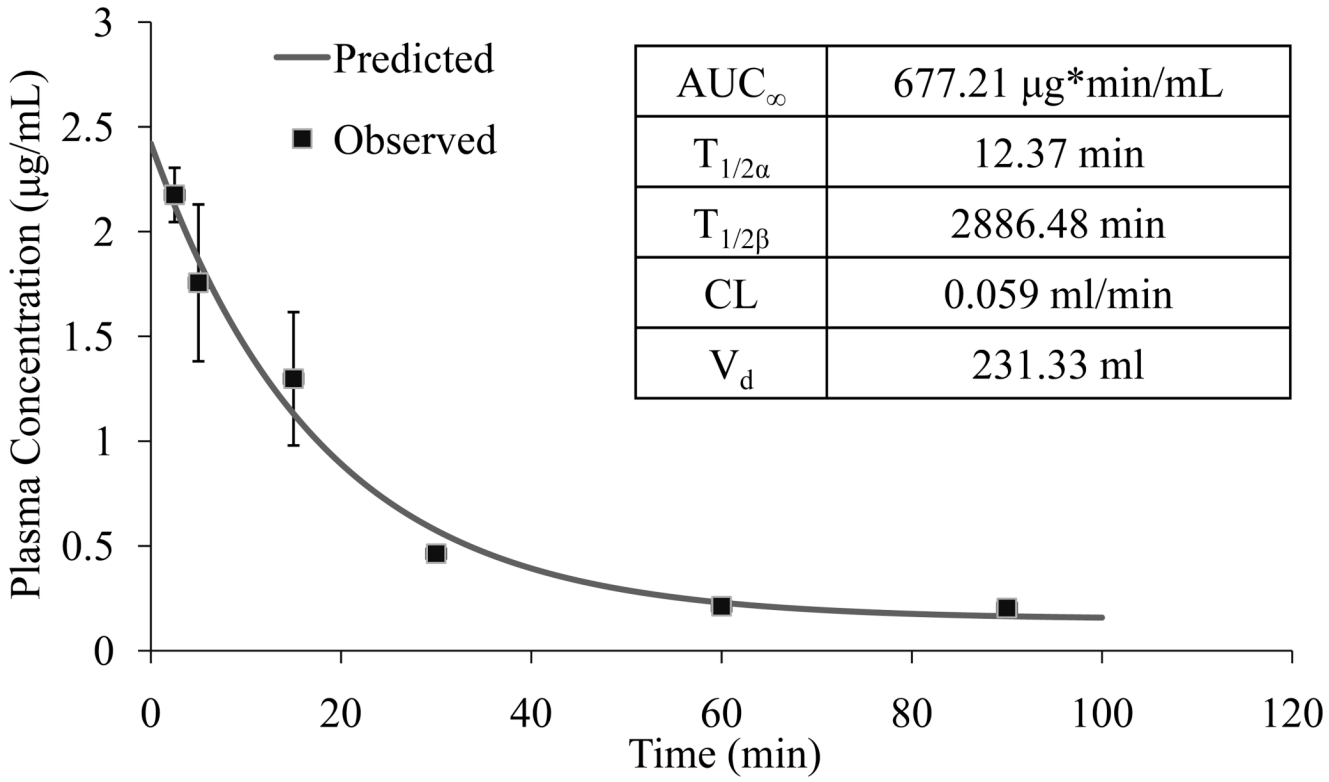

AUC_{∞}	677.21 μg*min/mL
$T_{1/2\alpha}$	12.37 min
$T_{1/2\beta}$	2886.48 min
CL	0.059 ml/min
V_d	231.33 ml

Figure 9.
Pharmacokinetic profiles of M6P-GFLG-HPMA-GFLG-^{32}P-TFO at 30min after post vein injection. Plasma data was analyzed using a two-compartment model with WinNonlin Enterprise (version 5.2) software. AUC = Area under the curve; CL = Clearance; V_d = Volume of distribution.

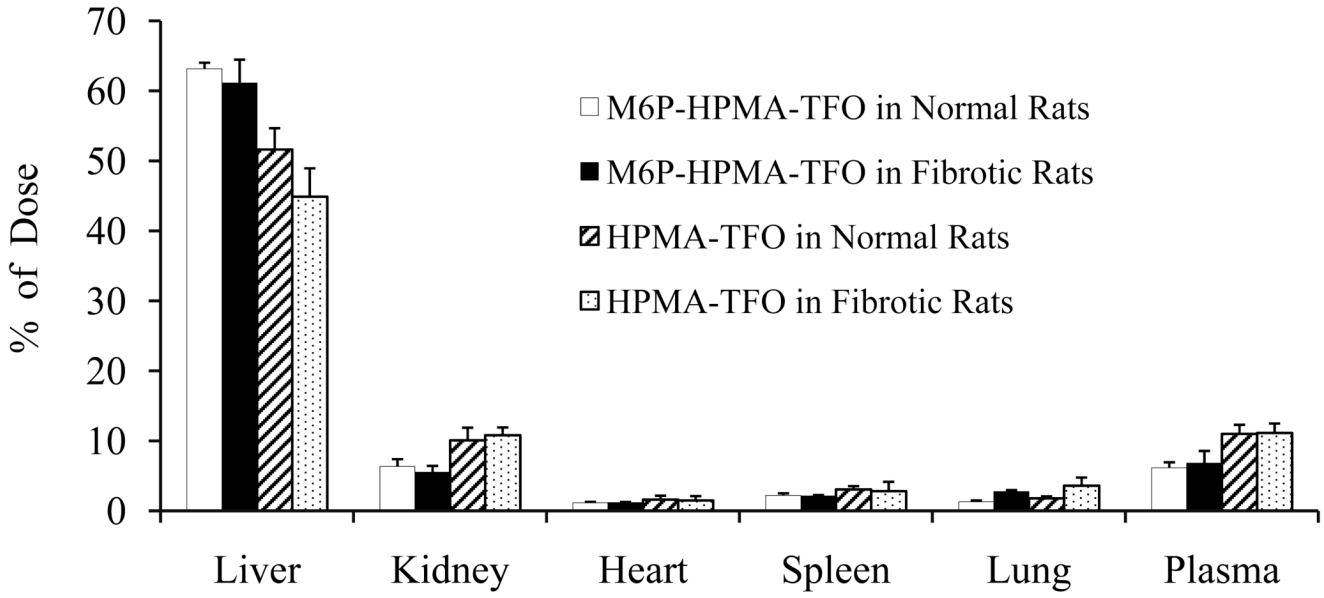

Figure 10.

Effect of fibrosis on hepatic uptake of M6P-GFLG-HPMA-GFLG-^{32}P-TFO and HPMA-^{32}P-TFO after systemic administration into DMN induced fibrotic rats. At 30 min postinjection of this conjugate (1×10^{6}cpm) at a dose of 0.2mg/kg, blood was collected by cardiac puncture. Rats were sacrificed; major organ were isolated, washed with saline and subjected into scintillation counter. Values are the mean ± S.D. of 3 rats.

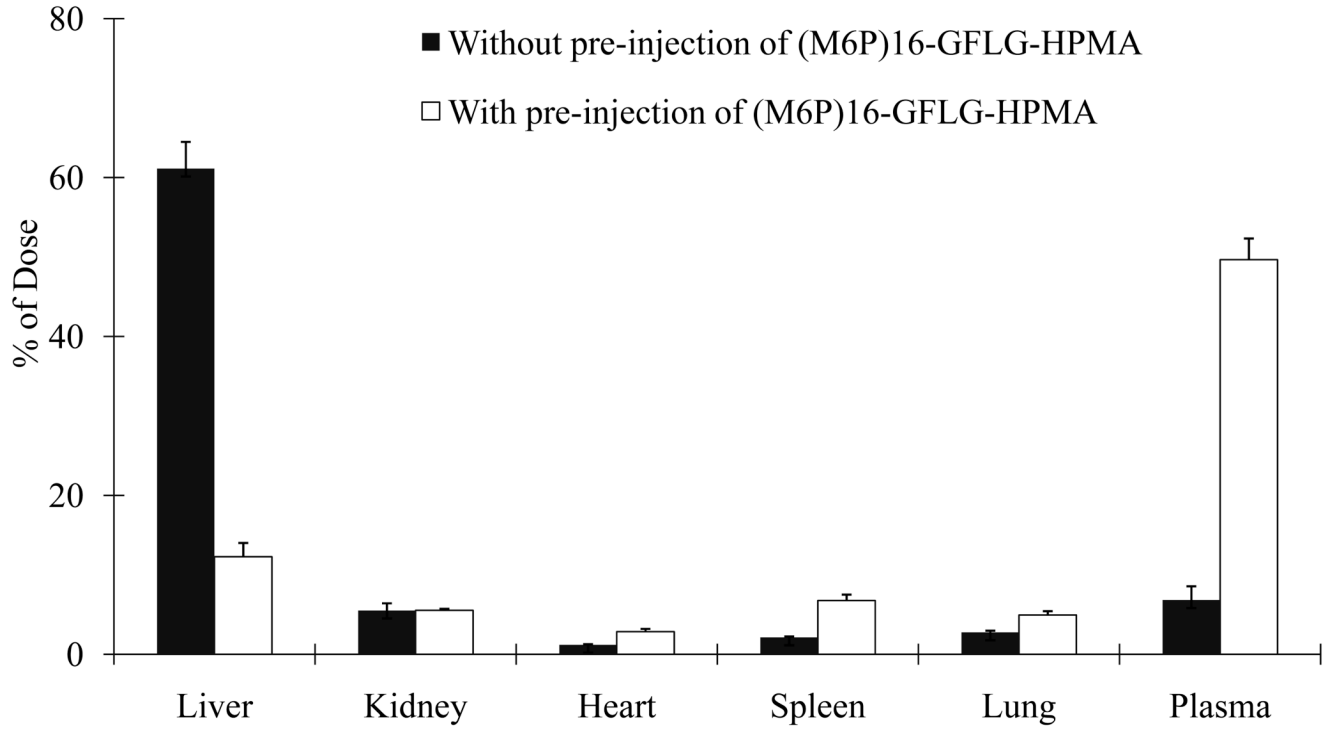

Figure 11.
Effect of excess M6P-GFLG-HPMA on the biodistribution of M6P-GFLG-HPMA-GFLG-^{32}P-TFO in fibrotic rats.

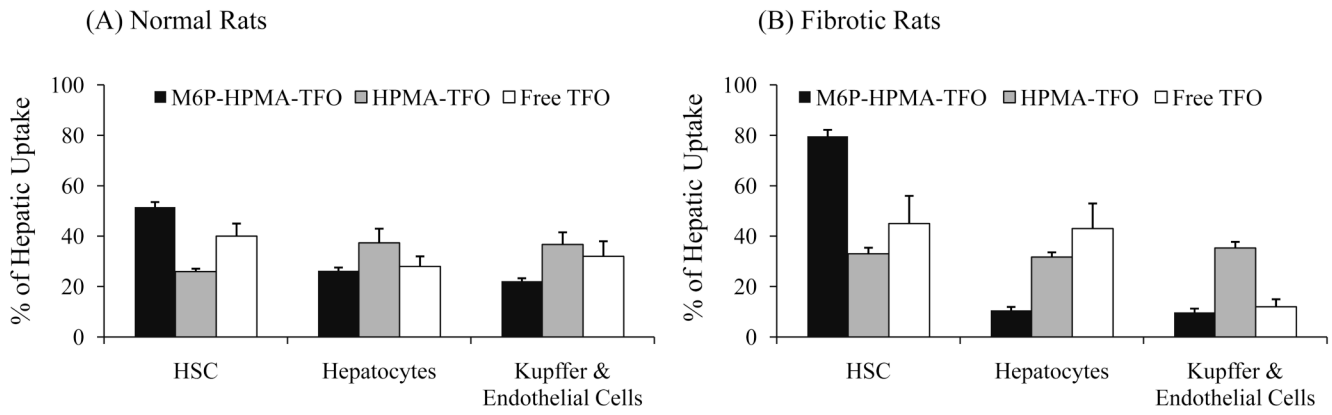

Figure 12.

Intrahepatic distribution of M6P-GFLG-HPMA-GFLG-^{32}P-TFO in normal and fibrotic rats. The liver was perfused in situ by collagenase/pronase digestion at 30 min post-injection of M6P-GFLG-HPMA-GFLG-^{32}P-TFO, HPMA-GFLG-^{32}P-TFO or ^{32}P-TFO at dose of 0.2 mg TFO/kg of body weight. Hepatocytes, Kupffer and endothelial cells, and hepatic stellate cells (HSC) were separated and the associated radioactivity was measured. The contribution of each liver cell type was exposed as percentage of total liver uptake. Results are expressed as the mean ± S.D. (n=3).

Table 1

Tissue Uptake Rate Index and Clearance of ^{32}P-TFO and M6P-GFLG-HPMA-GFLG-^{32}P-TFO after systemic Administration into Rats

Sample	AUC_{90} (μg*min/mL)	Tissue uptake rate index (μL/h/g)					Organ clearance (μL/h)				
		Liver	Kidney	Heart	Spleen	Lung	Liver	Kidney	Heart	Spleen	Lung
Conjugate	67.11	2176	1033	578	1146	450	11531	1137	318	436	383
		±58	±391	±31	±68	±112	±308	±430	±17	±26	±26
TFO	95.15	376	235	49	205	55	2218	241	23	83	42
		±38	±29	±3	±10	±9	±206	±41	±2	±7	±8